Writhe of center vortices and topological charge: An explicit example

Falk Bruckmann*

*Instituut-Lorentz for Theoretical Physics, Universiteit Leiden, P.O. Box 9506, NL-2300 RA Leiden,
The Netherlands*

Michael Engelhardt†

Institut für Theoretische Physik, Universität Tübingen, Auf der Morgenstelle 14, 72076 Tübingen, Germany

The manner in which continuum center vortices generate topological charge density is elucidated using an explicit example. The example vortex world surface contains one lone self-intersection point which contributes a quantum 1/2 to the topological charge. On the other hand, the surface in question is orientable and thus must carry global topological charge zero due to general arguments. Therefore, there must be another contribution, coming from vortex writhe. The latter is known for the lattice analogue of the example vortex considered, where it is quite intuitive. For the vortex in the continuum, including the limit of an infinitely thin vortex, a careful analysis is performed and it is shown how the contribution to the topological charge induced by writhe is distributed over the vortex surface.

I. INTRODUCTION

Chromomagnetic center vortex degrees of freedom [1] furnish the basis for one of the most attractive paradigms of the strong interaction vacuum, the center vortex picture. Using the model assumption that the two-dimensional closed vortex world surfaces can be regarded as random surfaces in four-dimensional (Euclidean) space-time, the principal phenomena characterizing low-energy strong interaction physics can be successfully described, i.e., confinement, the spontaneous breaking of chiral symmetry and the axial $U_A(1)$ anomaly [2–4]. This picture was inspired and is corroborated by lattice experiments [5–9] in which the vortex content of lattice Yang-Mills configurations is extracted and subsequently used to assess the significance of the vortex degrees of freedom for the phenomenology of the strong interaction vacuum.

In particular, the gluonic topological charge entering the $U_A(1)$ anomaly can be understood in terms of the topology of the vortex world surfaces [3,4,10–12]. Topological charge associated with center vortex world surfaces is generated in two different ways, self-intersections of the surfaces and writhe. In realistic random surface ensembles, the latter is statistically by far the more important [3,13].

On the other hand, the intuition gained hitherto from considering lattice-generated "cubistic" vortex surfaces [3,4,12] can be misleading when trying to understand the more subtle writhe of continuum vortex surfaces. To understand why, consider as a simple two-dimensional analogue the continuum and lattice versions of a "figure 8," i.e., a closed self-intersecting line in a plane, as shown in Fig. 1. As will be discussed below, in four dimensions, lattice topological charge appears where *the set of tangent vectors to the vortex*

spans all four dimensions of space-time. In the two-dimensional analogue of Fig. 1, the tangent vectors to the figure 8 span both dimensions of the plane at the self-intersection point, where two branches of the line provide two linear independent tangent vectors. In addition, this is true for all the corners of the lattice figure 8, since the line bends in an abrupt way, resulting in two linearly independent tangent vectors from one branch (as limits from "before" and "after" the point). Such a behavior is the analogue of writhe in the case of four-dimensional thin lattice vortices. However, at first sight, it does not seem to be present for the continuum figure 8, where the tangent space is of course one-dimensional everywhere except at the self-intersection point.

The purpose of the present paper is to provide a simple, pedagogical, explicit example of a continuum vortex configuration illustrating how topological charge density arises. In particular, the contribution from vortex writhe is elucidated. It turns out that continuum writhe is spread smoothly over the surface and arises in connection with certain combinations of *gradients of the tangent vectors*.

The example to be discussed here is formulated within the framework of $SU(2)$ gauge theory. The gluonic fields of this particular example will, however, point into a fixed color direction throughout space-time. Thus, the problem to be treated below is essentially an Abelian one.
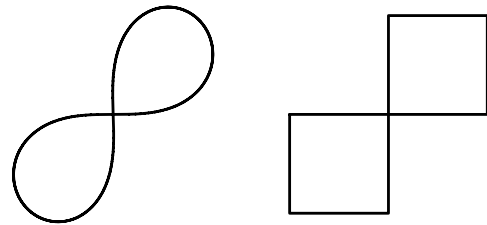

FIG. 1. Left: Continuum figure 8 in a plane (e.g., a lemniscate); right: coarse-grained lattice figure 8.

---

*Email address: bruckmann@lorentz.leidenuniv.nl

†Email address: engelm@tphys.physik.uni-tuebingen.de

FIG. 4. Continuous, gradual time dependence of a vortex loop going through the stages depicted in Fig. 3, but without discontinuous changes in the shape of the loop as time evolves.

simultaneously twist the bottom of it in a corkscrew motion around a vertical axis by the angle π, while holding the top fixed ($t=-0.9$ through $t=-0.3$). Then let the vortex line intersect itself, as depicted by the images at $t=-0.3$ through $t=0.3$. Afterwards, twist again by the angle π such that the shapes at the times $t=0.3$ through $t=0.9$ are mirror images of the shapes seen at the corresponding times $-t$, cf. Fig. 4. Thus, one arrives again at a simple planar loop which then closes. Note that in the representation of Fig. 4, and also of Fig. 5, in the last stage of the time evolution it is the top of the loop which is corkscrewed back into the (approximately fixed) bottom part. If one, however, considers the *relative* motion of the bottom with respect to the top, one sees that the bottom rotates with respect to the top by the angle π *in the same direction* as in the initial stage. The writhe in this configuration, to be discussed in detail further below, comes from this 2π rotation of the two ends of the loop with respect to each other; such a rotation of course is only possible if one concomitantly allows the loop to self-intersect once. As will be exhibited explicitly below, these two actions are each associated with topological charge contributions of modulus 1/2, which cancel each other to give global topological charge zero.

As the second step towards a smooth continuum surface, all that remains is to smoothen out the corners of the loops depicted in Fig. 4, cf. Fig. 5. This completes the construction of a smooth continuum analogue of the lattice surface[2] shown in Fig. 2. A convenient parametrization of the com-
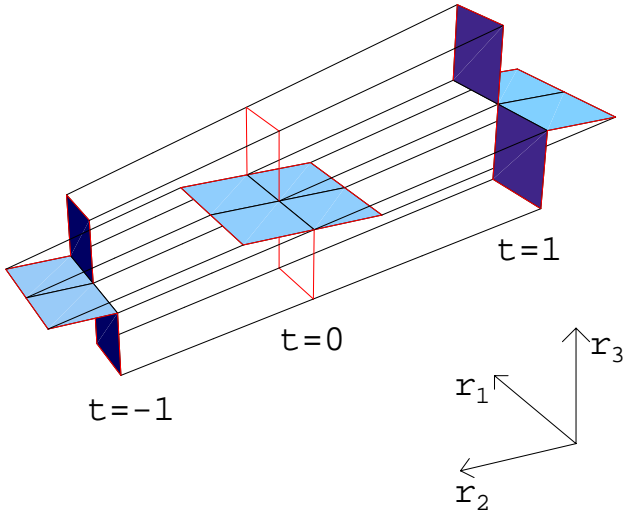

FIG. 2. Example vortex world-surface configuration composed of elementary squares on a (Euclidean) four-dimensional hypercubic lattice, taken from [3]. At each lattice time slice, $t \in \{-1,0,1\}$, shaded squares are part of the vortex surface. These squares are, furthermore, connected to squares running in the time direction; their location can be inferred most easily by keeping in mind that each edge (lattice link) of the configuration is connected to exactly two squares, i.e., the surface is closed. The surface possesses one isolated point at which it self-intersects, at the center of the configuration, and has no self-intersection lines. Note that the two non-shaded squares at $t=0$ are *not* part of the vortex; only the two sets of three links bounding them are. These are slices at $t=0$ of surface segments running in time direction from $t=-1$ through to $t=1$; sliced at $t=0$, these surface segments show up as lines.

II. DESCRIPTION OF THE VORTEX WORLD-SURFACE

Consider the vortex world-surface depicted in Fig. 2, which was first introduced in [3] and subsequently also studied in [12]. It is composed of elementary squares on a (Euclidean) four-dimensional hypercubic lattice. Due to the coarse-grained nature of the underlying lattice, changes in the vortex shape as time evolves can only take place abruptly, at the times $t=-1,0,1$, cf. Fig. 3.

As a first step towards finding a continuum analogue, make the time evolution gradual,[1] as depicted in Fig. 4.

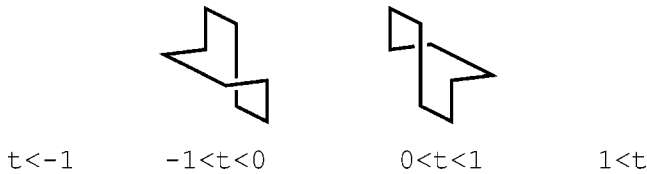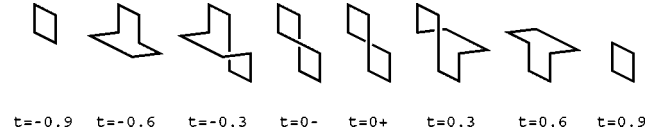In other words, open a planar loop and then pull and

FIG. 3. Viewing the vortex world surface depicted in Fig. 2 in terms of the time evolution of a vortex line in three-dimensional space, there are only four distinct stages of the time evolution, during which the vortex shape remains constant.
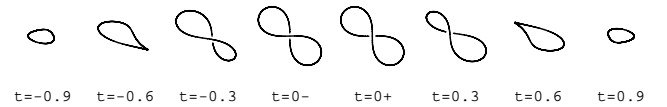

FIG. 5. Spatial shape of the loop displayed in Fig. 4 smoothed out to yield an altogether smooth vortex world surface. A gif movie of the complete time evolution of the vortex loop can be downloaded by visiting the abstract page of Ref. [25] and following the instructions in the Comments section there.

---

[1]A similar, but not identical, smoothing of the time evolution was considered in [12].

[2]Note that the discussion of topological charge in [10] is in some respects too restricted in that it does not encompass the smooth continuum surface discussed here, which contains a single intersection point. In [10], it is assumed that intersection points of smooth surfaces occur in pairs. The formulation in the published version of [10] is already sufficiently careful to take into account the lattice version, Fig. 2, by allowing for other singular points on surfaces besides intersection points. Singular points are those points where the tangent vectors to the vortex configuration span all four dimensions of space-time.

plete world surface is the following (the source of this parametrization will be further commented upon below):

$$y(s_1,s_2) = \sqrt{\sin 2s_2} \begin{pmatrix} -\cos s_1 \ (\cos s_2 + \sin s_2)/\sqrt{2} \\ -\cos s_1 \ (\cos s_2 - \sin s_2)/\sqrt{2} \\ -\sin s_1 \ \cos s_2 \\ \sin s_1 \ \sin s_2 \end{pmatrix},$$

$$s_1 \in [0, 2\pi], \quad s_2 \in [0, \pi/2]. \tag{1}$$

In fact, Fig. 5 was generated using this parametrization; details on how to extract closed vortex loops in three-dimensional space from Eq. (1) at fixed times $t \equiv y_1(s_1, s_2)$ are given in Appendix A. In plotting Fig. 5, the viewing angle of the observer at the different times displayed was adjusted such as to best match the viewing angle of Figs. 2–4. The world-surface parametrized by Eq. (1) will serve to illustrate how topological charge density arises from writhe of smooth continuum vortex surfaces, which is the central objective of the present work.

Specifying the space-time location of the vortex world surface does not completely determine a vortex configuration. It does determine the structure of the moduli of the gluonic field strength tensor components, $\text{Tr}_{color} F_{\mu\nu}^2$, for each μ, ν, which are concentrated on the vortex surface in a way which will be described more explicitly in the next section; however, it still leaves the color direction of the field strength tensor components, $F_{\mu\nu}^a$, free. Even if one assumes F^a to be aligned with the three-direction in color space,[3] $F^a = F \delta^{a3}$, then there still remains a freedom in the sign of F, which can be viewed as a choice of the *orientation* of the vortex world surface.

Orientation can be assigned to a surface by locally associating a sense of curl with the surface elements it is made up of. The reader is invited to do so with the surface of Fig. 2; for each elementary square making up the surface, define a curl in the sense of a definite order of running around the four edges of the square. If it is possible to define curls for all squares such that all pairs of squares sharing an edge (i.e. neighbors) display matching orientation, then the surface is orientable. I.e., its global structure does not impose frustrations on the attempt to align all neighboring surface elements, or in other words, the attempt to *orient* the surface. This can be verified for the surface shown in Fig. 2, and it is equally true for the (topologically equivalent) surface parametrized by Eq. (1).

In terms of the associated vortex field strength, which will be constructed explicitly in the next section, orienting the surface implies that the field strength behaves in a continu-

---

[3]Since at generic points on a vortex surface, there is only one nonvanishing field strength tensor component (details follow later), this can usually be achieved via a gauge transformation, which will be assumed to have been done within the present treatment. The field strength associated with the vortex world surface (1) constructed explicitly further below will indeed be of the form $F^a = F \delta^{a3}$.

ous manner as one moves about the surface. By contrast, lines on the surface at which the orientation flips would correspond to Dirac magnetic monopole singularities [10]. A non-orientable surface structure actually forces the presence of monopoles in the associated gauge field; however, also orientable surfaces can carry monopoles (voluntarily, so to speak), if one chooses not to consistently orient the surface but instead allows for lines on the surface at which the orientation, i.e. the sign of the vortex field strength, flips.

The vortex surface parametrized by Eq. (1) can also be arrived at directly in the continuum, completely independent of the above connection to a lattice surface. Namely, it results when casting a perturbed instanton into the Laplacian center gauge, albeit with monopoles present on the surface (which in fact is necessary in order to generate the unit topological charge of the instanton). This is explained in more detail in Appendix B. In the treatment below, on the other hand, no flips of orientation of the field strength will be present on the (orientable) vortex surface parametrized by Eq. (1). The field strength will thus behave smoothly as one moves about the surface. As a result of this simpler behavior of the gluonic color vector, the configuration will carry *global* topological charge zero. In fact, it is quite generally the case that oriented vortex world surfaces are associated with vanishing global topological charge [10]. One way of seeing this is to recast the global topological charge as an integral over the boundary of the space-time manifold under consideration [14]. In [10], a construction of the vortex gauge field was given in which this gauge field has support on a three-volume bounded by the vortex surface, and with no Dirac string singularities in the gauge field *as long as the vortex surface is orientable*. Thus, for orientable compact vortex surfaces (and correspondingly compact three-volumes spanning them), the gauge field vanishes at the boundary of space-time and there are no interior boundaries due to the absence of Dirac strings; therefore, the global topological charge vanishes. By contrast, non-oriented vortex surfaces force the presence of Dirac strings, thus providing the possibility of nonvanishing topological charge via contributions from interior integration boundaries.

III. FIELD STRENGTH AND TOPOLOGICAL CHARGE

Chromomagnetic center vortices carry a field strength concentrated on the vortex, where the nonvanishing field strength tensor component is the one associated with the two space-time directions locally perpendicular to the vortex surface. Given a surface parametrization $y(s) = y(s_1, s_2)$ such as (1), a corresponding field strength can be constructed explicitly as

$$F_{\mu\nu}(x) = \frac{\pi \sigma^3}{2} \epsilon_{\mu\nu\kappa\lambda} \int d^2 s \Sigma_{\kappa\lambda}(s) f[x - y(s)] \tag{2}$$

with $d^2s = ds_1 ds_2$ and the (oriented) surface element

$$\Sigma_{\kappa\lambda}(s) \equiv \epsilon_{ab} \frac{\partial y_\kappa}{\partial s_a} \frac{\partial y_\lambda}{\partial s_b} \tag{3}$$

where ϵ_{ab} represents the usual two-dimensional antisymmetric symbol with $\epsilon_{12}=1$. Due to the combination of the two tangent vectors to the surface, $\partial y/\partial s_1$ and $\partial y/\partial s_2$ in Eq. (3), with the ϵ symbol in (2), the nonvanishing field strength tensor component is thus indeed the one associated with the two space-time directions locally perpendicular to the vortex surface. For instance, a surface locally running in the 1-2 directions carries Σ_{12} and therefore F_{34}. On the other hand, σ^3 denotes the third Pauli matrix, encoding the color structure of the vortex. Note thus that the field strength to be used here points into a constant direction in color space, $F^a = F\delta^{a3}$, rendering the present problem essentially Abelian.[4] Finally, the *profile function f* in (2) provides the freedom to vary the transverse structure of the vortex field strength, since it controls the value of the field strength at finite distances $|x-y(s)|$ from the surface parametrized by $y(s)$. To preserve the total flux carried by the vortex when f is varied, f must be normalized,

$$\int d^4z f(z) = 1. \tag{4}$$

To be definite, below a (four-dimensional) Gaussian profile function

$$f(z) = \frac{1}{a^4\pi^2} e^{-z^2/a^2} \tag{5}$$

will be used, with the variable a controlling the thickness of the vortex; in the limit $a\rightarrow 0$, Eq. (5) reduces to a four-dimensional delta function,

$$\lim_{a\rightarrow 0} f(z) = \delta^4(z). \tag{6}$$

This corresponds to the limit of an infinitely thin vortex. For the moment, the vortices will in fact be taken to be infinitely thin, even though realistic, physically relevant vortices are not infinitely thin, but thick in the sense that the field strength is smeared out to the vicinity of every point $y(s)$. Further below, a thickening of the vortices will indeed play a crucial role in resolving the subtleties involved in evaluating the topological charge density arising from writhe of a thin vortex world surface.

Two more remarks about the field strength (2) are in order before proceeding. For one, a proper field strength must satisfy continuity of flux, i.e., the Bianchi identity,

$$\epsilon_{\rho\tau\mu\nu}\partial_\tau F_{\mu\nu}=0 \tag{7}$$

where it has already been used that the problem is essentially an Abelian one. The field strength (2) satisfies (7), for any profile function f, as sketched in Appendix C. Secondly, the normalization of (2) has been adequately chosen such that the vortex indeed carries flux corresponding to the center of

the $SU(2)$ gauge group [10], i.e., a Wilson loop circumscribing the vortex yields the phase -1. This is demonstrated in Appendix D.

The topological charge Q and the corresponding topological charge density $q(x)$ are defined as

$$Q = \frac{1}{32\pi^2}\int d^4x\, \epsilon_{\mu\nu\kappa\lambda} \text{Tr}\, F_{\mu\nu}F_{\kappa\lambda} \equiv \int d^4x\, q(x). \tag{8}$$

In view of this expression, topological charge density is generated at those points in space-time where there are nonvanishing field strength tensor components $F_{\mu\nu}$, $F_{\kappa\lambda}$ such that the indices $\{\mu,\nu,\kappa,\lambda\}$ span all four space-time directions. Translating this (naively) into the properties of (thin) vortex surfaces, in view of the discussion so far, the same must hold for the surface elements $\Sigma_{\mu\nu}$, $\Sigma_{\kappa\lambda}$ of the vortex. In other words (in analogy to the two-dimensional toy model of the Introduction), topological charge is ostensibly generated at those points in space-time where the set of tangent vectors to a thin vortex surface configuration spans all space-time directions [3].

This way of stating the characteristics of a vortex surface necessary for generating topological charge is quite adequate in some circumstances. For example, as will be seen in the example discussed below, for lattice surfaces it is entirely sufficient, and technically convenient, to consider idealized, infinitely thin surfaces for the purpose of evaluating the topological charge,[5] and to look for the points where the set of tangent vectors spans all four space-time directions. Furthermore, even when considering general continuum vortex surfaces, *intersection points* are adequately described by this characterization. For instance, a surface locally running into the 1-2 directions carries F_{34}; a surface locally running into the 3-4 directions carries F_{12}. If the two happen to intersect at a point, the product $F_{12}F_{34}$ is nonvanishing and topological charge is generated. Such intersection points will be present for lattice surfaces as well as thin and thick vortices in the continuum (where the surfaces need not cross perpendicularly). They always contribute $\pm 1/2$ to the topological charge (even when the crossing is not perpendicular [10]), where the sign just depends on the relative orientation of the surfaces.

On the other hand, one must not be too naive in applying the above characterization, in the case of general continuum surfaces, to other contributions to the topological charge, which will be subsumed under the term *writhing* contributions.[6] The corresponding topological charge density is rather hidden in the singular nature of the field strength

---

[4]In particular, also the gauge field generating the vortex field strength (2) can be constructed to point into the three-direction in color space [10].

[5]Note also that the global topological charge can be recast as an integral over the boundary of the space-time manifold under consideration [14]; therefore, it should be independent of any specific assumptions about the vortex transverse profile, which, after all, merely corresponds to a local deformation of the gauge field in the vicinity of the vortex.

[6]Writhe is a property of loops in three dimensions which enters the topological charge in a $(3+1)$-dimensional picture [10].
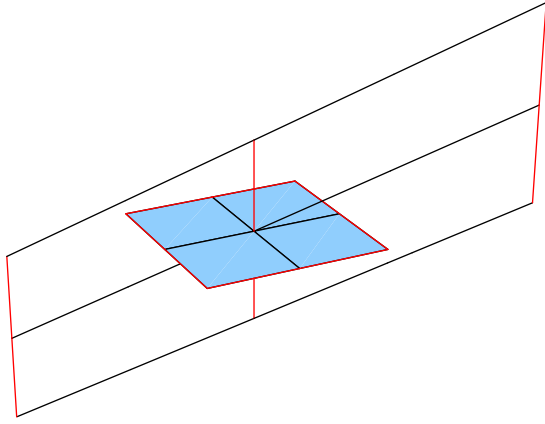
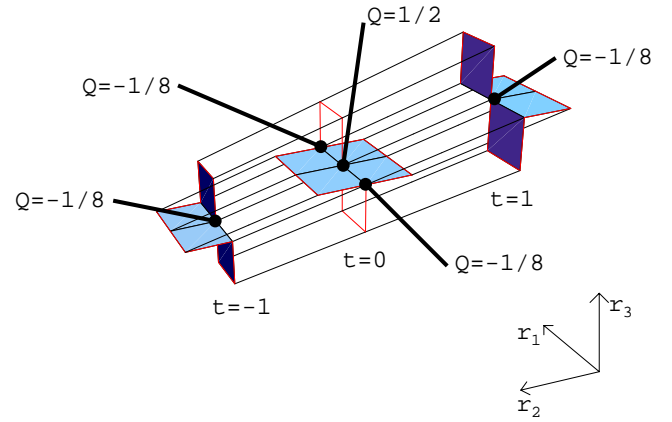FIG. 6. Detailed view of the intersection point in Fig. 2.

FIG. 7. Topological charge contributions from vortex self-intersection and writhe present in the world surface depicted in Fig. 2. To fully determine the signs of the contributions, the relative orientations of the elementary squares making up the surface must be fixed; this was done (starting from an initial square of arbitrary orientation) in such a way as to completely orient the surface, i.e., there are no edges shared by two squares at which the orientation flips.

associated with a thin continuum vortex surface, as will be discussed in detail further below. As a result, it is easily missed if one naively just looks for those points in the surface configuration where the set of tangent vectors spans all four space-time directions. It is the main objective of this work to elucidate the writhing contributions using the example surfaces which were introduced in Sec. II.

A. Lattice surface

As already mentioned above, finding the set of points where the tangent vectors to the surface configuration span all four space-time directions is sufficient to capture all contributions to the topological charge in the case of lattice surfaces made up of elementary squares. In this case, the topological charge density is concentrated at lattice sites; each instance of two squares sharing a lattice site and their combined tangent vectors spanning all four space-time directions contributes a "quantum" $\pm 1/32$ to the topological charge [3]. As before, the sign depends on the relative orientation of the squares.

Considering the lattice configuration of Fig. 2, one notices a self-intersection point at the center of the configuration with $Q=1/2$. This contribution results from four elementary squares connected to the intersection point extending into the 1-2 directions and four elementary squares connected to the intersection point extending into the 3-4 directions, cf. the detailed view displayed in Fig. 6. This indeed amounts to 16 pairs of perpendicular squares, i.e., $Q=16/32=1/2$.

The complete set of topological charge contributions associated with the surface depicted in Fig. 2 is shown in Fig. 7. Thus, apart from the intersection point at the center of the configuration, there are four writhing contributions concentrated at other lattice sites. At those sites, the vortex surface bends in such a way that it generates the perpendicular squares needed for a topological charge contribution within one single branch of the surface. A closer look reveals that there are four pairs of perpendicular squares at each such point, i.e., topological charge contributions $Q=4\times(-1/32)=-1/8$. Together, these writhing contributions exactly cancel the one from the intersection point, such that $Q_{global}=1/2-4/8=0$. This is in agreement with the general statement that oriented vortex world-surfaces are associated with

vanishing global topological charge [10].

Note thus that, on the lattice, writhe is concentrated at points on the vortex surface. For smooth continuum surfaces, the topological charge density associated with writhe will be spread out smoothly on the surfaces corresponding to the more gradual way in which they twist; this will become clear in the subsequent sections.

B. Continuum surface

Having discussed the topological charge of the coarse-grained lattice surface displayed in Fig. 2, one may ask how this treatment translates to the continuum analogue parametrized by Eq. (1). If one again starts from the statement that topological charge is generated where the tangent vectors to the surface span all four space-time directions, the contribution from the intersection point is as evident as before. However, one may be (mis-) led to conclude that there are no further contributions; after all, in the case of a smooth continuum surface, away from self-intersection points, there is always a well-defined unique two-dimensional tangent plane at each point. Nowhere do the tangent vectors span all four space-time directions. Where is the contribution from vortex writhe?[7]

Clearly, it would be too naive to declare it absent; for one, the smooth configuration shown in Fig. 5 is topologically equivalent to the lattice version depicted in Fig. 2. Also on general grounds, an orientable surface such as the one of Fig. 5 must have global topological charge zero [10]; therefore, there *must* be writhing contributions canceling the contribution from the self-intersection point which is certainly there. The point is that the writhing contributions are rather hidden

---

[7]The authors acknowledge R. Bertle for insisting this question be answered, thus sparking the present investigation.

in the singular structure of the field strength corresponding to an infinitely thin vortex surface, which has been implicitly assumed in the above discussion.

To properly extract the writhing contributions, one must view the infinitely thin vortex surfaces as an idealized limiting case of general thick vortices (in fact, physically relevant vortices have a finite thickness). When the vortex field strength is smeared out transversally, there will of course in general be a certain overlap between field strengths originating from the smearing of neighboring points on the original thin surface. This leads to a nonvanishing topological density $\epsilon_{\mu\nu\kappa\lambda}F_{\mu\nu}F_{\kappa\lambda}$ even if the underlying thin surface is smooth, as long as it curves suitably, i.e. writhes, in the space-time region under consideration. If one now makes the vortices thinner, then the overlap regions shrink, but at the same time, the modulus of the field strength increases such that in the thin limit, a finite topological density remains on the thin vortex surface. This in fact must happen such that the global topological charge is entirely independent of the vortex thickness, including the infinitely thin limit—after all, an topological quantity should be independent of local deformations such as a thickening of the vortex. The main purpose of the present treatment lies in demonstrating all this explicitly using the specific example vortex world surface introduced in Eq. (1). First, thick vortices will be treated, in which the width of the profile functions a, cf. Eq. (5), can still be varied. Then, the thin limit $a \to 0$ will be considered.

1. Thick vortex

Inserting the field strength (2) into the topological charge density (8), one obtains

$$q(x) = \frac{1}{16} \int d^2s \int d^2s' \, \epsilon_{\rho\tau\beta\gamma} \Sigma_{\rho\tau}(s) \Sigma_{\beta\gamma}(s')$$

$$\times f[x-y(s)]f[x-y(s')] \quad (9)$$

after having taken the color trace, $\text{Tr}(\sigma^3 \sigma^3) = 2$, and having simplified the Lorentz structure with the help of

$$\epsilon_{\mu\nu\kappa\lambda}\epsilon_{\mu\nu\rho\tau}\epsilon_{\kappa\lambda\beta\gamma} = 2(\delta_{\kappa\rho}\delta_{\lambda\tau} - \delta_{\kappa\tau}\delta_{\lambda\rho})\epsilon_{\kappa\lambda\beta\gamma} = 4\epsilon_{\rho\tau\beta\gamma}. \quad (10)$$

Appendix E contains the tedious, but straightforward, algebra involved in inserting the specific parametrization (1) into the surface elements and subsequently reducing (9) to

$$q(x) = \frac{1}{4} \int d^2s \int d^2s' f[x-y(s)]f[x-y(s')]$$

$$\times [\sin 2s_2 \sin 2s_2' \sin^2(s_1-s_1')$$

$$- \sin 3(s_2-s_2') \sin(s_2-s_2')]. \quad (11)$$

To proceed from this simple form for the topological density, explicit profile functions f must be inserted. Using Eq. (5), one needs to evaluate the convolution of the Gaussian profile functions in order to obtain the topological charge $\int d^4x q(x)$,

$$\int d^4x f[x-y(s)]f[x-y(s')]$$

$$= \frac{1}{4\pi^2 a^4} \exp\left[-\frac{1}{a^2}\left(\frac{1}{2}(y(s))^2\right.\right.$$

$$\left.\left. + \frac{1}{2}(y(s'))^2 - y(s)y(s')\right)\right]$$

$$= \frac{1}{4\pi^2 a^4} \exp\left[-\frac{1}{a^2}\left(\frac{1}{2}\sin 2s_2 + \frac{1}{2}\sin 2s_2'\right.\right.$$

$$\left.\left. - \sqrt{\sin 2s_2 \sin 2s_2'}\cos(s_2-s_2')\cos(s_1-s_1')\right)\right]$$

$$(12)$$

where the parametrization (1) has been put in. Inspecting Eqs. (11) and (12), one notices that the topological charge is now an integral over s, s' in which the integrand depends only on the difference $s_1 - s_1'$, and not on the individual angles. Therefore, by substituting $p = s_1 - s_1'$ and $q = s_1 + s_1'$, with the Jacobian $dp\,dq = 2ds_1\,ds_1'$, one can carry out one of the integrations via the general identity

$$\int_0^{2\pi} ds_1 \int_0^{2\pi} ds_1' g(s_1-s_1') = \frac{1}{2}\int_{-2\pi}^{2\pi} dp\, g(p) \int_{|p|}^{4\pi-|p|} dq$$

$$= 2\int_0^{2\pi} dp\, g(p)(2\pi-p), \quad (13)$$

where in the last equality, the p-integration interval has been halved using the fact that in the case considered here, $g(p) \equiv g(|p|)$. Combining Eqs. (11), (12) and (13), the topological charge reduces to

$$Q = \frac{1}{8\pi^2 a^4} \int_0^{\pi/2} ds_2 \int_0^{\pi/2} ds_2' \int_0^{2\pi} dp [\sin 2s_2 \sin 2s_2' \sin^2 p$$

$$- \sin 3(s_2-s_2')\sin(s_2-s_2')](2\pi-p)$$

$$\times \exp\left[-\frac{1}{a^2}\left(\frac{1}{2}\sin 2s_2 + \frac{1}{2}\sin 2s_2'\right.\right.$$

$$\left.\left. - \sqrt{\sin 2s_2 \sin 2s_2'}\cos(s_2-s_2')\cos(p)\right)\right]. \quad (14)$$

This integral is easily evaluated numerically for diverse a, and always vanishes, independent of the choice of a, as was to be expected from the discussion of the lattice version of the vortex surface in the previous section. Therefore, the integral must include writhing contributions which serve to cancel the contribution of the self-intersection point at the center of the surface configuration.

In order to exhibit the writhe in more detail, it is useful to evaluate the topological charge density $q(x)$ numerically for a thick vortex profile and visualize the result. For this pur-

FIG. 8. Time slices of the topological charge density induced by the vortex field strength (2) with the vortex world-surface parametrization (1) and a vortex thickness of $a=1/5$, cf. (5). At the times $t=-0.9$ (left) and $t=-0.6$ (right), all points in space are plotted at which the modulus of the topological charge density $|q(x)|$ exceeds unity. At the two times displayed, these are actually all points with $q(x)<-1$; in the companion figure, Fig. 9, depicting further time slices, points with $q(x)>1$ will also be seen. To guide the eye, also the corresponding time slices of the thin vortex world-surface parametrization are plotted, identical to the plots in Fig. 5 at the corresponding times. Thus, the viewing angle of the observer matches the one adopted in Fig. 5.

pose, it is useful to rewrite Eq. (11). Working with Eq. (11), one would need to evaluate a four-dimensional integral for each space-time point x; however, the task can be greatly simplified by decomposing the square brackets in Eq. (11) using

$$\sin^2(s_1-s_1')=\frac{1}{2}(1-\cos 2s_1\cos 2s_1'-\sin 2s_1\sin 2s_1')$$

$$\sin 3(s_2-s_2')\sin(s_2-s_2')$$

$$=(\sin 3s_2\cos 3s_2'-\cos 3s_2\sin 3s_2')$$

$$\times(\sin s_2\cos s_2'-\cos s_2\sin s_2'). \tag{15}$$

By multiplying out all the terms which thus result in the square brackets and letting the integrations act on them separately, the topological charge density reduces to a sum over terms in which the four-dimensional integrals factorize into pairs of two-dimensional integrals over the unprimed and the primed variables, respectively.

Using this numerically convenient form, the topological charge density was evaluated for a grid of points in space at selected times $t\equiv x_1$, where, to be definite, the value $a=1/5$ was used in the profile functions f, cf. Eq. (5). In order to visualize the result, all points in space were plotted at which the modulus of the topological charge density exceeds a certain value, namely $|q(x)|>1$, for each time t. The results are displayed in Figs. 8–10.

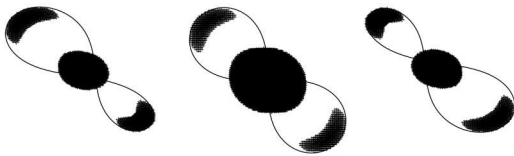At the times $t=-0.3,0,0.3$, one finds a round lump of topological charge density $q(x)>1$ near the center of the

FIG. 9. As Fig. 8, at the times $t=-0.3$ (left), $t=0$ (center) and $t=0.3$ (right). At these times, both points with $q(x)>1$ (at the center of the configuration, induced by the vortex self-intersection), and points with $q(x)<-1$ (kidney-shaped lumps at the periphery of the configuration, induced by vortex writhe) are present.

FIG. 10. As Fig. 8, at the times $t=0.6$ (left) and $t=0.9$ (right).

configuration; this is the contribution from the smeared-out intersection point. Furthermore, there are peripheral kidney-shaped lumps with $q(x)<-1$. Also the lumps seen at $t=-0.9,-0.6,0.6,0.9$ are associated with $q(x)<-1$. These are all the topological charge contributions induced by vortex writhe; they are evidently spread out smoothly over much of the vortex world surface (and its surroundings), corresponding to the smooth, gradual way in which the surface writhes. Careful evaluation of the topological charge density using thickened vortices thus allows one to recover all contributions to the topological charge, consistent with the lattice analysis and general arguments. Smoothness of a vortex surface does not preclude writhing contributions, as may have been thought from naively considering infinitely thin surfaces from the start, cf. the discussion at the beginning of Sec. III B. Below, it will be shown that the writhing contributions persist for infinitely thin vortex surfaces, by explicitly taking the limit of a vanishing thickness, $a\rightarrow 0$.

2. Thin vortex

Inspecting the expressions (9) or (11) for the topological charge density, taking the thin vortex limit implies that contributions to $q(x)$ can only come from points in the s,s' integrals where $y(s)=y(s')$, since the profile functions become δ distributions in this limit. In the case of the surface parametrization (1), the condition $y(s)=y(s')$ can be realized in two ways; either $s=s'$, corresponding to writhing contributions, or $(s_2,s_2')\in\{(0,\pi/2),(\pi/2,0)\}$ corresponding to the intersection point at $y=0$ (note that $s_2=s_2'\in\{0,\pi/2\}$ is already included in the former case). Thus, in the space of parameters s,s', the self-intersection contribution is conveniently isolated from the writhe, $s=s'$, and the corresponding regions in the integral over s,s' can be treated separately.

Consider first the self-intersection point. In this case, as already mentioned further above, one can work directly with thin vortices from the start, i.e., one can straightforwardly substitute $f(z)=\delta^4(z)$ in Eq. (11),

$$q(x)=\frac{1}{4}\int d^2s\int d^2s'\,\delta^4[x-y(s)]\delta^4[y(s)-y(s')]$$

$$\times[\sin 2s_2\sin 2s_2'\sin^2(s_1-s_1')$$

$$-\sin 3(s_2-s_2')\sin(s_2-s_2')] \tag{16}$$

where x has also been substituted by $y(s)$ in the second δ function in view of the presence of the first one. Now, consider in particular the integration region where s_2 is in the vicinity of 0 and s_2' is in the vicinity of $\pi/2$. In this limit, the

square brackets in Eq. (16) reduce to unity; furthermore, substituting $s_2=\rho^2/2$ and $s_2'=(\pi-\rho'^2)/2$, one has

$$y(s_1,\rho^2/2)=\rho\begin{pmatrix} -\cos s_1/\sqrt{2} \\ -\cos s_1/\sqrt{2} \\ -\sin s_1 \\ 0 \end{pmatrix}$$

$$y(s_1',(\pi-\rho'^2)/2)=\rho'\begin{pmatrix} -\cos s_1'/\sqrt{2} \\ \cos s_1'/\sqrt{2} \\ 0 \\ \sin s_1' \end{pmatrix} \qquad (17)$$

respectively, to leading order in ρ,ρ', where $s_1,s_1'\in[0,2\pi]$ as before. Therefore, (16) reduces to

$$q(x)=\frac{1}{4}\int ds_1 ds_1' d\rho d\rho' \rho\rho' \delta^4[x-y(s_1,\rho^2/2)]$$

$$\times\delta[-(\rho\cos s_1-\rho'\cos s_1')/\sqrt{2}]$$

$$\times\delta[-(\rho\cos s_1+\rho'\cos s_1')/\sqrt{2}]$$

$$\times\delta(-\rho\sin s_1)\delta(-\rho'\sin s_1') \qquad (18)$$

where the integrations over the (positive) variables ρ,ρ' cover the vicinity of $\rho,\rho'=0$. Going to Cartesian coordinates, $w_1=\rho\cos s_1$, $w_2=\rho\sin s_1$, and correspondingly for the primed variables, one ends up with

$$q(x)=\frac{1}{4}\int dw_1 dw_2 dw_1' dw_2'$$

$$\times\delta^4[x-y(s_1(w_1,w_2),s_2(w_1,w_2))]$$

$$\times\delta[-(w_1-w_1')/\sqrt{2}]\delta[-(w_1+w_1')/\sqrt{2}]$$

$$\times\delta(-w_2)\delta(-w_2')=\frac{1}{4}\delta^4(x). \qquad (19)$$

Supplementing this with the integration region in Eq. (16) where the roles of s and s' are interchanged, i.e., the former is in the vicinity of $\pi/2$ and the latter in the vicinity of 0, one obtains the same contribution again; thus, the topological charge density associated with the vortex self-intersection point altogether is

$$q_{int}(x)=\frac{1}{2}\delta^4(x). \qquad (20)$$

Correspondingly, by integrating over space-time, one obtains a contribution $Q_{int}=1/2$ to the global topological charge from the vortex self-intersection point. Note that, in the case of the intersection point, it was possible to work with thin vortices from the start and the application of the formalism was straightforward, yielding the correct result. In the case of the writhing contributions, on the other hand, this is not the case; the formalism becomes ambiguous if one naively uses

thin vortices. To see this, consider again Eq. (16). In the case $s=s'$, the term in the square brackets vanishes, corresponding to the fact that the tangent space at any point of a smooth surface is two-dimensional[8] (away from self-intersection points). On the other hand, when $s=s'$, the argument of the second δ function, $\delta^4[y(s)-y(s')]$, vanishes on a whole two-dimensional sub-manifold of space-time. Two out of the four dimensions in this δ function suffice to enforce $s=s'$, while the remaining two stay as $\delta^2(0)$. This is precisely the situation discussed in the initial remarks of Sec. III B; the product of these two factors is ambiguous, and one has to work to higher order in the thickness of the vortex in order to obtain a well-defined limit and thus properly extract the writhing contributions. Starting again from Eq. (11), one can write, in the limit $a\to0$,

$$q(x)=\frac{1}{4}\int d^2s\,\delta^4[x-y(s)]\int d^2s'f[y(s)-y(s')]$$

$$\times[\sin 2s_2\sin 2s_2'\sin^2(s_1-s_1')$$

$$-\sin 3(s_2-s_2')\sin(s_2-s_2')]. \qquad (21)$$

Note thus that $f[x-y(s)]$ in (11) has already been substituted by its thin limit, $\delta^4[x-y(s)]$; this will be justified *a posteriori* by the integral over s' in Eq. (21) yielding a well-defined result. Correspondingly, in the remaining profile function f in (21), x has again been substituted by $y(s)$ due to the presence of $\delta^4(x-y(s))$. Now, since the writhing contributions originate from the region around $s=s'$, it is useful to substitute

$$s_a'=s_a+r_a \qquad (22)$$

and to expand in the small quantities r_a; the profile function f will restrict the new r_a-integrations to small r_a when the vortex thickness a becomes small. To second order in the r_a, the square bracket in Eq. (21) reads

$$\sin 2s_2\sin 2(s_2+r_2)\sin^2 r_1-\sin 3r_2\sin r_2$$

$$=r_1^2\sin^2 2s_2-3r_2^2+O(r^3). \qquad (23)$$

Furthermore, the profile function f depends on $[y(s)-y(s')]^2$, which to this order reads

$$[y(s)-y(s')]^2=\left(\frac{\partial y(s)}{\partial s_a}r_a\right)^2+O(r^3)$$

$$=r_1^2\sin 2s_2+\frac{r_2^2}{\sin 2s_2}+O(r^3) \qquad (24)$$

as can be verified straightforwardly by computing the scalar products of the gradient vectors $\partial y(s)/\partial s_a$, cf. Eqs. (E3), (E4). As a consequence, the topological charge density reduces to

---

[8]Note that, also in the general expression (9), the combination $\epsilon_{\rho\tau\beta\gamma}\Sigma_{\rho\tau}(s)\Sigma_{\beta\gamma}(s')$ is easily seen to vanish when $s=s'$.

$$q(x) = \frac{1}{4} \int d^2 s \, \delta^4[x - y(s)] \frac{1}{a^4 \pi^2} \int dr_1 dr_2$$

$$\times \exp\left[-\frac{1}{a^2}\left(r_1^2 \sin 2s_2 + \frac{r_2^2}{\sin 2s_2} \right) \right]$$

$$\times (r_1^2 \sin^2 2s_2 - 3r_2^2). \tag{25}$$

In the limit $a \to 0$, the Gaussian strongly suppresses the integrand for increasing r_1, r_2, so that the integration ranges of r_1, r_2 can be extended over the whole real axis without incurring an error (except possibly for the boundary values $s_2 = 0$ and $s_2 = \pi/2$, at which the integral will be defined by continuity and will presently be seen to vanish). Furthermore, the higher order terms in the r_a which have been neglected above only lead to corrections which vanish as $a \to 0$. Evaluating the Gaussian integrals in Eq. (25), one arrives at

$$q_{writhe}(x) = \int d^2 s \, \delta^4[x - y(s)]\left(-\frac{1}{4\pi}\sin 2s_2 \right). \tag{26}$$

Thus, the topological charge density originating from vortex writhe persists in the thin limit; it is concentrated on the vortex surface and, in view of $(y(s))^2 = \sin 2s_2$, grows as the square of the distance from the origin, consistent with the visualization for thick vortices exhibited in Figs. 8–10. The authors checked that the same result is obtained using a (properly normalized) Lorentzian for the profile function f. Furthermore, by integrating (26) over space-time, one obtains a writhing contribution to the global topological charge

$$Q_{writhe} = -\frac{1}{4\pi}\int_0^{2\pi} ds_1 \int_0^{\pi/2} ds_2 \sin 2s_2 = -\frac{1}{2}, \tag{27}$$

which exactly cancels the contribution from the self-intersection point Q_{int}, as expected.

As a last point, it will be sketched how the above computation of the writhing contribution can be generalized beyond the specific example considered here, i.e., starting from the general expression (9) instead of (11) and taking the limits $s' \to s$, $a \to 0$ in analogy to Eqs. (21)–(26). The general form analogous to Eq. (25) reads

$$q(x) = \int d^2 s \, \delta^4[x - y(s)]\frac{1}{16 a^4 \pi^2} \int d^2 r [0 + O(r) + h^{ab} r_a r_b$$

$$+ O(r^3)] \exp(-g^{ab} r_a r_b / a^2) \tag{28}$$

where the leading term is always absent due to the geometry of the expression for the topological charge density, i.e., the combination $\epsilon_{\rho\tau\beta\gamma}\Sigma_{\rho\tau}(s)\Sigma_{\beta\gamma}(s)$, cf. Eq. (9), vanishes identically.[9] Here, the induced metric and a bilinear in gradients of the surface elements have been introduced,

___
[9]Note that the analogous term in the Yang-Mills action diverges as $1/a^2$, cf. [10,15].

$$g^{ab} \equiv \frac{\partial y_\mu}{\partial s_a}\frac{\partial y_\mu}{\partial s_b}, \quad h^{ab} \equiv \Sigma_{\mu\nu}\frac{\partial^2 \widetilde{\Sigma}_{\mu\nu}}{\partial s_a \partial s_b} = \frac{\partial \Sigma_{\mu\nu}}{\partial s_a}\frac{\partial \widetilde{\Sigma}_{\mu\nu}}{\partial s_b},$$

$$\widetilde{\Sigma}_{\mu\nu} \equiv \frac{1}{2}\epsilon_{\mu\nu\kappa\lambda}\Sigma_{\kappa\lambda} \tag{29}$$

respectively. To obtain the second expression for h^{ab}, it has been used that terms of the form $\epsilon_{\mu\nu\kappa\lambda}(\partial y_\mu/\partial s_a)(\partial y_\nu/\partial s_b)(\partial y_\kappa/\partial s_c)$ vanish for all λ, a, b, c since the derivatives contain either s_1 or s_2 twice, rendering the expression symmetric in the corresponding greek indices. The same argument is used again to arrive at (31) below. As before, only the terms written out explicitly in (28) are relevant and evaluate to

$$q(x) = \int d^2 s \, \delta^4[x - y(s)]\left(-\frac{1}{16\pi}h^{ab}\frac{\partial}{\partial g^{ab}}\frac{1}{\sqrt{g}} \right) \tag{30}$$

where $g = \det g^{ab}$. This is the generalization of Eq. (26), where, using the parametrization (1), g^{ab} and h^{ab} happen to be diagonal and $g = 1$. By virtue of the inverse metric g_{ab}, one finally arrives at [10]

$$q(x) = \frac{1}{32\pi}\int d^2 s \, \delta^4[x - y(s)]\left(\frac{1}{\sqrt{g}}g_{ab}\frac{\partial \Sigma_{\mu\nu}}{\partial s_a}\frac{\partial \widetilde{\Sigma}_{\mu\nu}}{\partial s_b} \right)$$

$$= \frac{1}{32\pi}\int d^2 s \sqrt{g}\, \delta^4[x - y(s)]g_{ab}\frac{\partial}{\partial s_a}\frac{\Sigma_{\mu\nu}}{\sqrt{g}}\frac{\partial}{\partial s_b}\frac{\widetilde{\Sigma}_{\mu\nu}}{\sqrt{g}}, \tag{31}$$

the latter being more natural from the reparametrization point of view (where $d^2 s \sqrt{g}$ and $\Sigma/\sqrt{g} = \epsilon_{ab}/\sqrt{g} \ldots$ are the proper objects). The space-time integral over this expression is known as a representation of (minus) the self-intersection number, which is thus given in terms of an integral over a smooth density [16]. In the context of the present work, this identification corresponds to the observation that the "smooth" writhing contribution to the topological charge cancels the "discrete" one from the self-intersection point. The validity of Eq. (31) has been corroborated in the present paper by considering the thick vortex explicitly.

There exists another intuitive formula for the self-intersection number in terms of normal gauge fields [17,18], which is related to the fact that $\widetilde{\Sigma}$ is normal to the vortex surface: Take two orthonormal normal vectors n^1 and n^2, and define an $SO(2)$ gauge field $A = n^1_\mu d n^2_\mu$ and its field strength $F = dA$. Then the self-intersection number is given by $\int F/4\pi$.

As is best seen from the appearance of $h \sim \partial \Sigma \partial \widetilde{\Sigma}$ in the equations above, the writhe is distributed according to the gradients of the tangent space and of the normal space, respectively. The vortex example discussed in this work is planar at the self-intersection point such that the writhing contribution vanishes there, but this will not be the case for arbitrary vortex surfaces.

IV. CONCLUDING REMARKS

Using a specific simple example, it has been shown in this work how topological charge arises through vortex writhe in the space-time continuum. The topological charge density was visualized for a thickened vortex and it was verified that the global topological charge is independent of the vortex thickness. Topological charge through writhe persists in the limit of arbitrarily thin vortex world surfaces, even though it is rather hidden in the singular nature of the vortex field strength in this limit. Smoothness of a vortex surface does not preclude these writhing contributions, which were demonstrated to be proportional to a particular combination of gradients of the surface elements,[10] i.e., of the tangent space.

In the example discussed here, the appearance of writhe and the existence of the self-intersection point are intertwined; a closed vortex surface not extending to infinity has to bend and "come back" in order to display a lone self-intersection point. This need not be the case when space-time possesses compact directions; the vortex surface can then be closed due to periodicity. Therefore, on the four-torus, one can have a (thin) vortex consisting of two branches $x_1 = x_2 = 0$ and $x_3 = x_4 = 0$ which intersect at a point but otherwise are completely planar. Then the contributions to the topological charge are $Q_{int} = 1/2$ and $Q_{writhe} = 0$. This does not contradict general statements on the quantization of topological charge; half-integer topological charges exist on the torus when accompanied by twisted boundary conditions.[11] On the four-torus a single self-intersection point can thus occur without writhe. Conversely, writhe can obviously exist without a self-intersection point, a simple example being the time evolution of Fig. 5 from $t = -0.9$ to $t = 0-$ followed by the time reversed process (i.e., the loop is unscrewed back in the direction it came from instead of being twisted further as in Fig. 5). Globally, this leads to $Q_{writhe} = 0$. An example of a (non-orientable) surface with writhing contribution $Q_{writhe} = 1/2$ and no intersection point is depicted in [4]. A smooth continuum analogue of this surface (as well as the precise relation to twisted boundary conditions) has not been given so far.

Two additional points became apparent in the course of this investigation which deserve mention. For one, comparing Secs. III A and III B, it is considerably simpler to evaluate the topological charge of a surface made up of elementary squares on a hypercubic lattice than to evaluate it for a general continuum surface, in which writhe is rather hidden, as already remarked further above. On the lattice, topological charge is concentrated at lattice sites as opposed to being smeared out over the surface; as a consequence, it is simply accessible by counting pairs of mutually orthogonal elemen-

tary squares meeting at the lattice sites, cf. also [3]. A viable and efficient procedure of determining the global topological charge of a general continuum surface indeed would lie in latticizing it, i.e. finding a topologically equivalent lattice surface on a suitably fine lattice, and evaluating its global topological charge instead.[12] Note that this stands in marked contrast to the usual statement made for lattice Yang-Mills configurations; on the standard Yang-Mills lattice, carrying Yang-Mills link variables, topological charge is much harder to define and detect than in the continuum, and indeed becomes an ambiguous quantity for generic Yang-Mills configurations. By contrast, on a lattice carrying vortex fluxes such as used here, which is dual to the standard Yang-Mills lattice, topological charge actually is easier to evaluate than in the continuum.

Finally, note that a standard way of capturing the topology of lines in three-dimensional space lies in defining a framing. As discussed, e.g. in [10], one constructs a second line displaced from the original one by a small distance; the two lines define the edges of a ribbon which may twist and writhe, with the two lines correspondingly entangled. With the help of such a framing, one can define a *three-dimensional* writhing number; the topological charge associated with the whole world surface of a vortex line can then be related to the difference between the three-dimensional writhing numbers at the initial and final times bounding the space-time region under consideration [10]. It would be interesting to reformulate this directly in four-dimensional space-time, since the procedure of defining a framing fits into the formalism used in the present work; it corresponds to one particular way of choosing the profile function f. Namely, the original infinitely thin vortex line at a given time is "smeared" into a ribbon, i.e. the δ-function profile is replaced by a profile with support on a short line in four-dimensional space.

The authors did not further explore this option, since the smoother profile functions used in the present treatment already permitted an entirely satisfactory definition of the topological density associated with writhing *in four dimensions*, summarized in the closed expression (31) for arbitrary smooth surfaces. For the purposes of the present investigation, smooth profile functions, leading to a finite gluonic field strength, were not only more appropriate from a technical point of view, but also more natural from a physics point of view; realistic physical vortices indeed possess thick, spread-out transverse profiles.

---

[10]Note that the mere existence of such gradients does not suffice; for instance, the 2-sphere embedded in R^4 possesses gradients of the surface elements, but the writhe vanishes.

[11]Indeed, the gauge fields corresponding to this configuration, $A_1 = \pi \Theta(x_2) \delta(x_1) \sigma^3$, $A_3 = \pi \Theta(x_4) \delta(x_3) \sigma^3$, $A_2 = A_4 = 0$ obey transition functions similar to the charge 1/2 instanton solutions of constant field strength [19,20].

[12]Note, however, that, as far as the local topological density is concerned, the (absolute values of) local contributions to the topological charge on rectangular lattices are bounded from below by the "quantum" 1/16 (not 1/32, because at the sites of a *closed* lattice surface, there cannot be a *single* pair of mutually perpendicular elementary squares). Therefore, to approximate continuum writhing contributions to the topological *density* to any precision, one has to use non-rectangular polygonal surfaces, which in the simplest case just corresponds to a triangulation of the continuum surface.

APPENDIX A: VORTEX LOOP AT FIXED TIME

In order to cast the parametrization (1),

$$y(s_1,s_2)=\sqrt{\sin 2s_2}\begin{pmatrix} -\cos s_1 & (\cos s_2+\sin s_2)/\sqrt{2} \\ -\cos s_1 & (\cos s_2-\sin s_2)/\sqrt{2} \\ -\sin s_1 & \cos s_2 \\ \sin s_1 & \sin s_2 \end{pmatrix}$$

in terms of the time evolution of a closed loop in three-dimensional space, as plotted in Fig. 5 for selected times t, one eliminates the parameter s_1 in favor of the time

$$\begin{aligned} t &\equiv y_1(s_1,s_2) \\ &= -\sqrt{\sin 2s_2}\cos s_1(\cos s_2+\sin s_2)/\sqrt{2} \quad \in[-1,1] \end{aligned} \tag{A1}$$

i.e.,

$$\cos s_1 = -\frac{\sqrt{2}t}{\sqrt{\sin 2s_2}(\cos s_2+\sin s_2)} \tag{A2}$$

$$\sin s_1 = \pm\sqrt{1-\cos^2 s_1} \tag{A3}$$

where both signs are relevant; the plus sign yields the solution found in the interval $s_1\in[0,\pi]$, whereas the minus sign yields the solution found in the interval $s_1\in[\pi,2\pi]$. Both solutions must be taken into account in order to reproduce the parametrization (1) in the entire interval $s_1\in[0,2\pi]$. Thus, one obtains the alternative parametrization

$$y(t,s_2)=\begin{pmatrix} t \\ t(\cos s_2-\sin s_2)/(\cos s_2+\sin s_2) \\ \mp\cos s_2\sqrt{\sin 2s_2-2t^2/(\cos s_2+\sin s_2)^2} \\ \pm\sin s_2\sqrt{\sin 2s_2-2t^2/(\cos s_2+\sin s_2)^2} \end{pmatrix} \tag{A4}$$

which, at fixed time t, parametrizes a closed loop via the parameter s_2, taking into account both choices of sign. Note that, for a given time t, the range of s_2 is no longer $s_2\in[0,\pi/2]$, as in the original parametrization (1), but it is in general restricted to a smaller interval by the requirement that the argument of the square roots in Eq. (A4) be positive, i.e.

$$2t^2\leqslant\sin 2s_2(\cos s_2+\sin s_2)^2=\sin 2s_2(1+\sin 2s_2). \tag{A5}$$

The condition thus reduces to a quadratic equation for $\sin 2s_2$; picking out the relevant solution by taking into account the requirement $|\sin 2s_2|\leqslant1$, Eq. (A5) is solved by

$$\sin 2s_2\geqslant\frac{1}{2}(\sqrt{1+8t^2}-1). \tag{A6}$$

Thus,

$$\begin{aligned} s_2\in\Bigg[&\frac{1}{2}\arcsin\frac{1}{2}(\sqrt{1+8t^2}-1), \\ &\frac{\pi}{2}-\frac{1}{2}\arcsin\frac{1}{2}(\sqrt{1+8t^2}-1)\Bigg] \end{aligned} \tag{A7}$$

at the time t.

APPENDIX B: CONTINUUM VORTEX FROM LAPLACIAN CENTER GAUGE INSTANTON

Abelian [21] and center [5] gauges are used to define magnetic monopoles and center vortices as defects of gauge fixings. In the particular cases of the Laplacian Abelian gauge [22] and the Laplacian center gauge [7], monopoles and vortices are defined, respectively, to be the nodes of the ground state of the covariant Laplacian $-D^2[A]$ (in the adjoint representation) and the set of points where the two lowest-lying eigenvectors of this operator are parallel. The ground state ϕ of $-D^2[A]$ in the background of a single instanton (in regular gauge) has been found [23] to be three-fold degenerate and of the form (1_2 denoting the 2×2 unit matrix)

$$\phi_a=r^2g^\dagger\sigma_a g, \quad g=(x_41_2+ix_a\sigma_a)/r \tag{B1}$$

near the four-dimensional origin. There, both the monopole and the vortex are located, degenerate to a pointlike defect.

In [24], it was shown that perturbing the instanton background A such that the ground state is perturbed as $\phi_3\rightarrow\phi_3-R^2\sigma_3$ gives rise to a monopole loop of radius R in the x_1x_2 plane.

For the center vortex, one considers in the same spirit the perturbation

$$\phi_1^{\text{pert}}=\phi_1+\sigma_3, \quad \phi_3^{\text{pert}}=\phi_3 \tag{B2}$$

where the relevant scale has been put to 1. Straightforward algebra shows that ϕ_1^{pert} and ϕ_3^{pert} are parallel at

$$\varphi_{12}-\varphi_{34}=\pi\bmod 2\pi, \quad r=\sqrt{\sin 2\theta} \tag{B3}$$

where double polar coordinates have been introduced,

$$x_\mu = r(\cos\theta\cos\varphi_{12}, \cos\theta\sin\varphi_{12},$$

$$\sin\theta\cos\varphi_{34}, \sin\theta\sin\varphi_{34}). \tag{B4}$$

This leaves

$$s_2 \equiv \theta \in [0,\pi/2], \quad s_1 \equiv (\varphi_{12}+\varphi_{34})/2 \in [0,2\pi] \tag{B5}$$

as free parameters. Up to rotations and inversions in space-time, this corresponds to the vortex surface parametrization of Eq. (1); namely, one must permute the 1-, 3- and 4-components as $(1,3,4)\rightarrow(4,1,3)$, and then rotate the resulting 1- and 2-components as $(x_1,x_2)\rightarrow((x_1-x_2)/\sqrt{2}, (-x_1-x_2)/\sqrt{2})$. Note that, without the latter rotation, the parametrization would have a more symmetric form; however, for the purposes of visualization, the choice of coordinates (1) is more advantageous. This simply amounts to a change in the point of view of the observer, not an actual change in the form of the vortex surface.

The monopole defined by ϕ_1^{pert} has to fulfill (B3) plus the condition $\theta=\pi/4$, i.e. it is a loop on the vortex which is as far away as possible from the origin. The monopole of ϕ_3^{pert} is still degenerate to the origin (but adding a perturbation to it lifts also this degeneracy while leading to similar vortex surfaces). For the present purposes, the detailed form of the monopole loops is not relevant; the monopole content of the configuration resulting from the above construction is not adopted in the body of this work. Only the surface (1), which in itself is orientable and thus is not forced to carry monopoles, is used, and endowed with an oriented, smooth field strength.

APPENDIX C: BIANCHI IDENTITY

The field strength (2) satisfies the Abelian Bianchi identity (7) independent of the profile function f. Inserting (2) into (7) and using $\epsilon_{\rho\tau\mu\nu}\epsilon_{\mu\nu\kappa\lambda}=2(\delta_{\rho\kappa}\delta_{\tau\lambda}-\delta_{\rho\lambda}\delta_{\tau\kappa})$, one arrives at

$$\epsilon_{\rho\tau\mu\nu}\partial_\tau F_{\mu\nu} = \pi\sigma^3\partial_\tau\int d^2s f[x-y(s_1,s_2)]$$

$$\times\left(\epsilon_{ab}\frac{\partial y_\rho}{\partial s_a}\frac{\partial y_\tau}{\partial s_b} - \epsilon_{ab}\frac{\partial y_\tau}{\partial s_a}\frac{\partial y_\rho}{\partial s_b}\right). \tag{C1}$$

Exchanging the dummy indices a,b in the second term in the parentheses using $\epsilon_{ba}=-\epsilon_{ab}$ and, furthermore, inserting

$$\frac{\partial y_\tau}{\partial s_b}\partial_\tau f[x-y(s_1,s_2)] = -\frac{\partial y_\tau}{\partial s_b}\frac{\partial}{\partial y_\tau}f[x-y(s_1,s_2)]$$

$$= -\frac{\partial}{\partial s_b}f[x-y(s_1,s_2)] \tag{C2}$$

yields

$$\epsilon_{\rho\tau\mu\nu}\partial_\tau F_{\mu\nu} = -2\pi\sigma^3\int ds_1 ds_2 \frac{\partial y_\rho}{\partial s_1}\frac{\partial}{\partial s_2}f(x-y)$$

$$+2\pi\sigma^3\int ds_1 ds_2 \frac{\partial y_\rho}{\partial s_2}\frac{\partial}{\partial s_1}f(x-y) \tag{C3}$$

after having written out the sums over a,b explicitly. Now, one can partially integrate the first term over s_2 and the second term over s_1 without generating surface contributions, upon which the two terms are seen to cancel, as was to be shown. When partially integrating over s_1, there is no surface contribution because $y(0,s_2)=y(2\pi,s_2)$ for any s_2. When partially integrating over s_2, both $y(s_1,0)=0$ and $y(s_1,\pi/2)=0$; therefore, also $\partial y_\rho/\partial s_1=0$ for $s_2=0,\pi/2$, i.e. the surface contribution already vanishes separately for these two values of s_2.

Note that this argument does not particularly depend on the specifics of the vortex surface considered here. Quite generally, since vortex world surfaces are closed, they can be viewed as "time" evolutions of closed loops. Therefore, one can choose[13] "time" as one parameter of the vortex surface, and an angle parametrizing the closed loop at a given "time" as the other. As a result, partial integration over the aforementioned angle never generates a surface contribution, since the two end points of the interval on which the angle is defined map to identical space-time points for any given "time." On the other hand, at the initial and final "times," the surface parametrization reduces to a point; otherwise, the surface would not be closed. In other words, at these two "times," the surface parametrization is a constant space-time point independent of the angle variable. As a result, the derivative of the parametrization with respect to the angle, which appears in the surface pieces under consideration [cf. the first term in Eq. (C3)], vanishes.

APPENDIX D: CENTER PHASE INDUCED BY VORTEX FLUX

To see that the normalization of (2) is adequately chosen such that vortices indeed carry flux corresponding to the center of the $SU(2)$ gauge group, consider for the sake of the argument a planar vortex world-surface extending into the 1-2-directions in space-time,

$$\bar{y}(s_1,s_2)=(s_1,s_2,0,0), \quad s_1,s_2\in[-\infty,\infty]. \tag{D1}$$

Any smooth vortex surface can be viewed as being locally planar, i.e. of the form (D1) on sufficiently small length scales (if the space-time axes are chosen suitably). Inserting (D1) into (2), one obtains the field strength

$$F_{34}(x)=\pi\sigma^3\int d^2s f[x-\bar{y}(s_1,s_2)] = \frac{\sigma^3}{a^2}e^{-(x_3^2+x_4^2)/a^2} \tag{D2}$$

where the explicit form (5) has been inserted. Now, consider a Wilson loop C located in the 3-4 plane circumscribing the vortex (e.g. a circle centered at the origin with sufficiently large radius R to capture the entire vortex flux, which may be smeared out via the profile function f; i.e., $R^2/a^2\gg 1$),

---

[13]This "time" does not have to correspond to physical time; also in the case of the parametrization (1), the parameter s_2 is not identical to physical time.

$$W[C] = \frac{1}{2} \operatorname{Tr} \exp\left(i \oint_C dx_\mu A_\mu \right) = \frac{1}{2} \operatorname{Tr} \exp\left(i \int_S dx_3 dx_4 F_{34} \right)$$

$$= \frac{1}{2} \operatorname{Tr} e^{i\pi\sigma^3} = -1. \tag{D3}$$

Here, for the second equality, Stokes' theorem has been used (in a fixed time slice, $x_1 = 0$), i.e. S represents the area in the 3-4 plane bounded by C. For the third equality, the condition $R^2/a^2 \gg 1$ has been used, which permits extending the integral over S to the entire 3-4 plane without appreciably changing the result. Note also that no path ordering is necessary in the Wilson loop due to the Abelian nature of the problem. Thus, one indeed has $W[C] = -1$, i.e. the total flux carried by the vortex corresponds to the nontrivial center element of the $SU(2)$ gauge group. Continuity of flux, i.e. the Bianchi identity (7), guarantees that this result extends to the entirety of any vortex world-surface given that it is true locally for a small vortex segment, as shown explicitly here.

APPENDIX E: SIMPLIFYING THE TOPOLOGICAL CHARGE DENSITY

The topological charge density (9),

$$q(x) = \frac{1}{16} \int d^2 s \int d^2 s' \, \epsilon_{\rho\tau\beta\gamma} \Sigma_{\rho\tau}(s) \Sigma_{\beta\gamma}(s')$$

$$\times f[x - y(s)] f[x - y(s')]$$

where, cf. (3),

$$\Sigma_{\kappa\lambda}(s) = \epsilon_{ab} \frac{\partial y_\kappa}{\partial s_a} \frac{\partial y_\lambda}{\partial s_b}$$

can be rewritten using

$$\epsilon_{\rho\tau\beta\gamma} \epsilon_{ab} \frac{\partial y_\rho(s)}{\partial s_a} \frac{\partial y_\tau(s)}{\partial s_b} = 2 \epsilon_{\rho\tau\beta\gamma} \frac{\partial y_\rho(s)}{\partial s_1} \frac{\partial y_\tau(s)}{\partial s_2} \tag{E1}$$

(and analogously for the sum over c,d in conjunction with the derivatives with respect to s'_c, s'_d) with the result

$$q(x) = \frac{1}{2} \int d^2 s \int d^2 s' f[x - y(s)] f[x - y(s')] \left[\left(\frac{\partial y_1(s)}{\partial s_1} \frac{\partial y_2(s)}{\partial s_2} - \frac{\partial y_2(s)}{\partial s_1} \frac{\partial y_1(s)}{\partial s_2} \right) \left(\frac{\partial y_3(s')}{\partial s'_1} \frac{\partial y_4(s')}{\partial s'_2} - \frac{\partial y_4(s')}{\partial s'_1} \frac{\partial y_3(s')}{\partial s'_2} \right) \right.$$

$$+ \left(\frac{\partial y_1(s)}{\partial s_1} \frac{\partial y_3(s)}{\partial s_2} - \frac{\partial y_3(s)}{\partial s_1} \frac{\partial y_1(s)}{\partial s_2} \right) \left(\frac{\partial y_4(s')}{\partial s'_1} \frac{\partial y_2(s')}{\partial s'_2} - \frac{\partial y_2(s')}{\partial s'_1} \frac{\partial y_4(s')}{\partial s'_2} \right)$$

$$\left. + \left(\frac{\partial y_2(s)}{\partial s_1} \frac{\partial y_3(s)}{\partial s_2} - \frac{\partial y_3(s)}{\partial s_1} \frac{\partial y_2(s)}{\partial s_2} \right) \left(\frac{\partial y_1(s')}{\partial s'_1} \frac{\partial y_4(s')}{\partial s'_2} - \frac{\partial y_4(s')}{\partial s'_1} \frac{\partial y_1(s')}{\partial s'_2} \right) \right] \tag{E2}$$

where the sums over $\rho, \tau, \beta, \gamma$ have been written out explicitly and the number of terms has been halved by using the freedom in exchanging the names of the dummy integration variables s, s'. Inserting the derivatives

$$\frac{\partial y(s_1, s_2)}{\partial s_1} = \sqrt{\sin 2s_2} \begin{pmatrix} \sin s_1 (\cos s_2 + \sin s_2)/\sqrt{2} \\ \sin s_1 (\cos s_2 - \sin s_2)/\sqrt{2} \\ -\cos s_1 \cos s_2 \\ \cos s_1 \sin s_2 \end{pmatrix} \tag{E3}$$

and

$$\frac{\partial y(s_1, s_2)}{\partial s_2} = \frac{1}{\sqrt{\sin 2s_2}} \begin{pmatrix} -\cos s_1 (\cos s_2 - \sin s_2)(1 + 4\cos s_2 \sin s_2)/\sqrt{2} \\ -\cos s_1 (\cos s_2 + \sin s_2)(1 - 4\cos s_2 \sin s_2)/\sqrt{2} \\ -\sin s_1 \cos s_2 (1 - 4\sin^2 s_2) \\ -\sin s_1 \sin s_2 (1 - 4\cos^2 s_2) \end{pmatrix} \tag{E4}$$

(where $\cos 2s_2$, $\sin 2s_2$ have been expanded in terms of $\cos s_2$, $\sin s_2$) into the six factors appearing in the square brackets in (E2), one has

$$\frac{\partial y_1(s)}{\partial s_1}\frac{\partial y_2(s)}{\partial s_2}-\frac{\partial y_2(s)}{\partial s_1}\frac{\partial y_1(s)}{\partial s_2}$$

$$=2\sin s_1\cos s_1\sin s_2\cos s_2 \qquad (E5)$$

$$\frac{\partial y_3(s')}{\partial s'_1}\frac{\partial y_4(s')}{\partial s'_2}-\frac{\partial y_4(s')}{\partial s'_1}\frac{\partial y_3(s')}{\partial s'_2}$$

$$=-2\sin s'_1\cos s'_1\sin s'_2\cos s'_2 \qquad (E6)$$

$$\frac{\partial y_1(s)}{\partial s_1}\frac{\partial y_3(s)}{\partial s_2}-\frac{\partial y_3(s)}{\partial s_1}\frac{\partial y_1(s)}{\partial s_2}$$

$$=-\frac{1}{\sqrt{2}}\cos s_2[\cos s_2(1-4\sin^2 s_2)$$

$$+\sin s_2(1-4\sin^2 s_2+2\cos^2 s_1)] \qquad (E7)$$

$$\frac{\partial y_4(s')}{\partial s'_1}\frac{\partial y_2(s')}{\partial s'_2}-\frac{\partial y_2(s')}{\partial s'_1}\frac{\partial y_4(s')}{\partial s'_2}$$

$$=\frac{1}{\sqrt{2}}\sin s'_2[-\sin s'_2(1-4\cos^2 s'_2)$$

$$+\cos s'_2(1-4\cos^2 s'_2+2\cos^2 s'_1)] \qquad (E8)$$

$$\frac{\partial y_2(s)}{\partial s_1}\frac{\partial y_3(s)}{\partial s_2}-\frac{\partial y_3(s)}{\partial s_1}\frac{\partial y_2(s)}{\partial s_2}$$

$$=-\frac{1}{\sqrt{2}}\cos s_2[\cos s_2(1-4\sin^2 s_2)$$

$$-\sin s_2(1-4\sin^2 s_2+2\cos^2 s_1)] \qquad (E9)$$

$$\frac{\partial y_1(s')}{\partial s'_1}\frac{\partial y_4(s')}{\partial s'_2}-\frac{\partial y_4(s')}{\partial s'_1}\frac{\partial y_1(s')}{\partial s'_2}$$

$$=\frac{1}{\sqrt{2}}\sin s'_2[-\sin s'_2(1-4\cos^2 s'_2)$$

$$-\cos s'_2(1-4\cos^2 s'_2+2\cos^2 s'_1)]. \qquad (E10)$$

Comparing the right-hand sides of Eqs. (E7) and (E9), one notices that they can be cast in the forms $(A+B)$ and $(A-B)$, respectively, with expressions A,B common to the two equations. Likewise, the right-hand sides of (E8) and (E10) can be cast in the forms $(C+D)$ and $(C-D)$, respectively, with common expressions C,D. As a result, after inserting (E7)–(E10), the second and the third lines in the square brackets in Eq. (E2) correspond to the forms $(A+B)(C+D)$ and $(A-B)(C-D)$, respectively, and therefore their sum simplifies to $(A+B)(C+D)+(A-B)(C-D)=2AC+2BD$. Thus, one has

$$q(x)=\frac{1}{2}\int d^2s\int d^2s'f[x-y(s)]f[x-y(s')]$$

$$\times\left[-\frac{1}{4}\sin 2s_1\sin 2s_2\sin 2s'_1\sin 2s'_2\right.$$

$$+\cos^2 s_2\sin^2 s'_2(1-4\sin^2 s_2)(1-4\cos^2 s'_2)$$

$$-\frac{1}{4}\sin 2s_2\sin 2s'_2(1-4\sin^2 s_2+2\cos^2 s_1)$$

$$\left.\times(1-4\cos^2 s'_2+2\cos^2 s'_1)\right] \qquad (E11)$$

where the third line corresponds to the combination $2AC$ referred to above, whereas the fourth and fifth lines correspond to $2BD$. Of course, the second line simply comes from the first line in the square brackets in (E2). To further simplify (E11), it is useful to substitute

$$\cos^2 z=(1+\cos 2z)/2 \qquad (E12)$$

$$\sin^2 z=(1-\cos 2z)/2 \qquad (E13)$$

everywhere (with z denoting any of the variables s_1,s'_1,s_2,s'_2). Multiplying out the resulting terms in the square brackets in (E11), one finds

$$q(x)=\frac{1}{8}\int d^2s\int d^2s'f[x-y(s)]f[x-y(s')]$$

$$\times[-\sin 2s_2\sin 2s'_2\sin 2s_1\sin 2s'_1+1$$

$$-(\cos 2s_2-\cos 2s'_2)-\cos 2s_2\cos 2s'_2-2\cos^2 2s_2$$

$$-2\cos^2 2s'_2-2\cos 2s_2\cos 2s'_2(\cos 2s_2-\cos 2s'_2)$$

$$+4\cos^2 2s_2\cos^2 2s'_2-\sin 2s_2\sin 2s'_2\cos 2s_1\cos 2s'_1$$

$$-2\sin 2s_2\sin 2s'_2(\cos 2s_2\cos 2s'_1-\cos 2s_1\cos 2s'_2)$$

$$+4\sin 2s_2\sin 2s'_2\cos 2s_2\cos 2s'_2] \qquad (E14)$$

where a factor four has been extracted from the square brackets. Now, all the terms inside the square brackets which are grouped into pairs by parentheses are seen to cancel if one uses the freedom to exchange the names of the dummy integration variables s,s' on one of the members of each pair. Furthermore, by using

$$\cos 2s_1\cos 2s'_1+\sin 2s_1\sin 2s'_1$$

$$=\cos 2(s_1-s'_1)=1-2\sin^2(s_1-s'_1) \qquad (E15)$$

to combine the first term of the first line and the second term of the fourth line in the square brackets in (E14), and supplementing this with the contribution $-\cos 2s_2\cos 2s'_2$ from the second line, one obtains

$$q(x) = \frac{1}{8} \int d^2s \int d^2s' f[x - y(s)] f[x - y(s')]$$

$$\times [2 \sin 2s_2 \sin 2s_2' \sin^2(s_1 - s_1') - \cos 2(s_2 - s_2')$$

$$+ \sin 4s_2 \sin 4s_2' + (1 - 2\cos^2 2s_2)(1 - 2\cos^2 2s_2')]$$

(E16)

after having combined the remaining terms in the first through fourth lines in the square brackets in (E14) into the product of parentheses in the last line of (E16). Again using (E12), this time with $z = 2s_2, 2s_2'$, one finally arrives at the result aimed for, Eq. (11),

$$q(x) = \frac{1}{4} \int d^2s \int d^2s' f[x - y(s)] f[x - y(s')]$$

$$\times [\sin 2s_2 \sin 2s_2' \sin^2(s_1 - s_1')$$

$$- \sin 3(s_2 - s_2') \sin(s_2 - s_2')]$$

after having used

$$\cos 4(s_2 - s_2') - \cos 2(s_2 - s_2')$$

$$= -2 \sin 3(s_2 - s_2') \sin(s_2 - s_2')$$

(E17)

and having extracted a factor two from the square brackets.

---

[1] G. 't Hooft, Nucl. Phys. **B138**, 1 (1978); H.B. Nielsen and P. Olesen, *ibid.* **B160**, 380 (1979); J. Ambjørn and P. Olesen, *ibid.* **B170**, 60 (1980); **B170**, 265 (1980).

[2] M. Engelhardt and H. Reinhardt, Nucl. Phys. **B585**, 591 (2000).

[3] M. Engelhardt, Nucl. Phys. **B585**, 614 (2000).

[4] M. Engelhardt, Nucl. Phys. **B638**, 81 (2002).

[5] L. Del Debbio, M. Faber, J. Greensite, and Š. Olejnik, Phys. Rev. D **55**, 2298 (1997); L. Del Debbio, M. Faber, J. Giedt, J. Greensite, and Š. Olejnik, *ibid.* **58**, 094501 (1998).

[6] P. de Forcrand and M. D'Elia, Phys. Rev. Lett. **82**, 4582 (1999).

[7] C. Alexandrou, M. D'Elia, and P. de Forcrand, Nucl. Phys. B (Proc. Suppl.) **83**, 437 (2000).

[8] K. Langfeld, O. Tennert, M. Engelhardt, and H. Reinhardt, Phys. Lett. B **452**, 301 (1999); M. Engelhardt, K. Langfeld, H. Reinhardt, and O. Tennert, Phys. Rev. D **61**, 054504 (2000).

[9] J. Greensite, Prog. Part. Nucl. Phys. **51**, 1 (2003).

[10] M. Engelhardt and H. Reinhardt, Nucl. Phys. **B567**, 249 (2000).

[11] J.M. Cornwall, Phys. Rev. D **61**, 085012 (2000); **65**, 085045 (2002).

[12] H. Reinhardt, Nucl. Phys. **B628**, 133 (2002).

[13] R. Bertle, M. Engelhardt, and M. Faber, Phys. Rev. D **64**, 074504 (2001).

[14] C. Itzykson and J.-B. Zuber, *Quantum Field Theory* (McGraw-Hill, Singapore, 1987).

[15] H. Kleinert, Phys. Lett. B **174**, 335 (1986).

[16] A.M. Polyakov, Nucl. Phys. **B268**, 406 (1986); S. K. Donaldson and P. B. Kronheimer, *The Geometry of Four-Manifolds* (Oxford University Press, Oxford, 1997).

[17] P.O. Mazur and V.P. Nair, Nucl. Phys. **B284**, 146 (1987).

[18] J. Pawelczyk, Int. J. Mod. Phys. A **11**, 2661 (1996).

[19] G. 't Hooft, Commun. Math. Phys. **81**, 267 (1981).

[20] P. van Baal, Commun. Math. Phys. **94**, 397 (1984).

[21] G. 't Hooft, Nucl. Phys. **B190**, 455 (1981).

[22] A.J. van der Sijs, Nucl. Phys. B (Proc. Suppl.) **53**, 535 (1997).

[23] F. Bruckmann, T. Heinzl, T. Vekua, and A. Wipf, Nucl. Phys. **B593**, 545 (2001).

[24] F. Bruckmann, J. High Energy Phys. **08**, 030 (2001).

[25] F. Bruckmann and M. Engelhardt, hep-th/0307219.